

We are IntechOpen, the world's leading publisher of Open Access books Built by scientists, for scientists

4,800

Open access books available

122,000

International authors and editors

135M

Downloads

Our authors are among the

154

Countries delivered to

TOP 1%

most cited scientists

12.2%

Contributors from top 500 universities

**WEB OF SCIENCE™**Selection of our books indexed in the Book Citation Index
in Web of Science™ Core Collection (BKCI)

Interested in publishing with us?
Contact book.department@intechopen.com

Numbers displayed above are based on latest data collected.

For more information visit www.intechopen.com

Electrocaloric Effect (ECE) in Ferroelectric Polymer Films

S. G. Lu¹, B. Rožič², Z. Kutnjak² and Q. M. Zhang¹

¹Materials Research Institute and Department of Electric Engineering,
The Pennsylvania State University, University Park, PA 16802

²Jozef Stefan Institute, 1000 Ljubljana

¹USA

²Slovenia

1. Introduction

The electrocaloric effect (ECE) is the change in temperature and/or entropy of a dielectric material due to the electric field induced change of dipolar states. Electrocaloric effect in dielectrics is directly related to the polarization changes under electric field.^[1-3,6] Hence a large polarization change is highly desirable in order to achieve a large ECE which renders the ferroelectric materials the primary candidates for developing materials with large ECE. Figure 1 illustrates schematically the ECE in a dipolar material. Application of an electric field to the material causes partial alignment of dipoles and consequently a reduction of entropy of the dipolar system. In an isothermal condition, the dipolar material rejects heat $Q=T\Delta S$ to the surrounding, where T is the temperature and ΔS is the isothermal entropy change. Or in an adiabatic process, to keep the total entropy of the material constant, the temperature of the dielectric is increased by ΔT , the adiabatic temperature change which is related to the $Q = C\Delta T$ where C is specific heat capacity of the dielectric. In a reverse process, as the applied electric field is reduced to zero and the dipoles return to the less ordered state (or disordered state), an increase in the entropy of dipolar system occurs and under an isothermal condition, the dielectric will absorb heat Q from the surrounding.

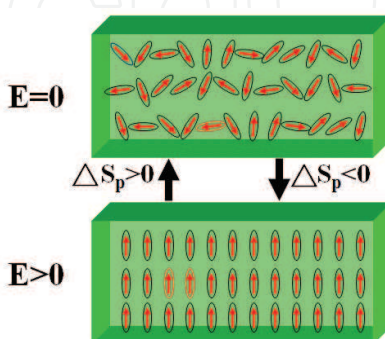


Fig. 1. Schematic drawing of the ECE process in a dipolar material. When $E=0$, the dipoles orient randomly. When $E > 0$, especially larger than the coercive electric field, the dipoles orient along the electric field direction.

The ECE may provide an effective means of realizing solid-state cooling devices for a broad range of applications such as on-chip cooling and temperature regulation for sensors or other electronic devices. Refrigerations based on ECE have the potential of reaching high efficiency relative to vapor-compression cycle systems, and no green house emission.

Solid-state electric-cooling devices based on the thermoelectric effect (Peltier effect) have been used for many decades (Spanner, 1951; Nolas, Sharp, and Goldsmid, 2001). However, these cooling devices require a large DC current which results in large amount of waste heat through Joule heating. For example, using the typical coefficient of performance (COP) for these devices, e.g. 0.4 to 0.7, 2.4 to 3.5 watts of heat will be generated at the hot end of the system when pumping 1 watt heat from the cold end. Hence, the thermoelectric effect based cooling devices will not meet the requirement of high energy efficiency.

A counterpart of ECE is the MCE, which has been extensively studied for many years due to the findings of giant magnetocaloric effect in several magnetic materials near room temperature (Gschneidner Jr., Pecharsky and Tsokol, 2005; Pecharsky, Holm, Gschneidner Jr. and Rink, 2003). Both ECE and MCE devices exploit the change of order parameter brought about by an external electric or magnetic field. However, the difficulty of generating high magnetic field for MCE devices to reach giant MCE, severely limits their wide applications. This makes the MCE devices difficult to be used widely, especially for miniaturized microelectronic devices, and to achieve high efficiency. In contrast, high electric field can be easily generated and manipulated, which makes ECE based cooling devices attractive and more practical for a broad range of applications.

This chapter will introduce the basic concept of ECE, the thermodynamic considerations on materials with large ECE, and review previous investigations on the ECE in polar crystals, ceramics, and thin films. A newly discovered large ECE in ferroelectric polymers will be presented. Besides, we will also discuss different characterization techniques of ECE such as the direct measurements and that deduced from Maxwell relations, as well as phenomenological theory on ECEs.

2. Thermodynamic considerations on materials with large ECE

2.1 Maxwell relations

In general the Gibbs free energy G for a dielectric material could be expressed as a function of temperature T , entropy S , stress X , strain x , electric field E and electric displacement D in the form

$$G = U - TS - X_i x_i - E_i D_i, \quad (1)$$

where U is the internal energy of the system, the stress and field terms are written using Einstein notation. The differential form of Eq. (1) could be written as

$$dG = -SdT - x_i dX_i - D_i dE_i. \quad (2)$$

Entropy S , strain x_i and electric displacement D_i can be easily expressed when the other two variables are assumed to be constant,

$$S = -\left(\frac{\partial G_1}{\partial T}\right)_{X,D}, x_i = -\left(\frac{\partial G_1}{\partial X_i}\right)_{T,D}, D_i = -\left(\frac{\partial G_1}{\partial E_i}\right)_{T,X}. \quad (3)$$

The Maxwell relation can be derived for (S, T) and (D, E) two pairs of parameters (Line and Glass, 1977),

$$\left(\frac{\partial S}{\partial E_i}\right)_{T,X} = \left(\frac{\partial D_i}{\partial T}\right)_{E,X}. \quad (4)$$

Or

$$\left(\frac{\partial T}{\partial E}\right)_S = \frac{T}{c_E} \left(\frac{\partial D}{\partial T}\right)_E = \frac{Tp_E}{c_E}, \quad (5)$$

where c_E is the heat capacity, p_E the pyroelectric coefficient. Eqs. (4) and (5) indicate the mutually inverse relationships of ECE and the pyroelectric coefficient. Hence, for the ECE materials with a constant stress X imparted, the isothermal entropy change ΔS and adiabatic temperature change ΔT can be expressed as (Line and Glass, 1977)

$$\Delta S = -\int_{E_1}^{E_2} \left(\frac{\partial D}{\partial T}\right)_E dE, \quad (6)$$

$$\Delta T = -\frac{T}{\rho} \int_{E_1}^{E_2} \frac{1}{c_E} \left(\frac{\partial D}{\partial T}\right)_E dE. \quad (7)$$

Equations (4) through (7) indicate that in order to achieve large ΔS and ΔT , the dielectric materials should possess a large pyroelectric coefficient over a relatively broad electric field and temperature range. For ferroelectric materials, a large pyroelectric effect exists near the ferroelectric (F) – paraelectric (P) phase transition temperature and this large effect may be shifted to temperatures above the transition temperature when an external electric field is applied. It is also noted that a large ΔT may be achieved even if ΔS is small when the c_E of a dielectric material is small. However, as will be pointed out in the following paragraph, this is not desirable for practical refrigeration applications where a large ΔS is required.

It is noted that in the temperature region including a first-order FE-PE transition, Eq. (6) should be modified to take into account of the discontinuous change of the polarization ΔD at the transition, i.e.,

$$\Delta S = -\int_0^E \left(\frac{dD}{dT}\right)_E dE + \Delta D \left(\frac{\partial E}{\partial T}\right). \quad (8)$$

Although a few studies on the ECE were conducted in which direct measurement of ΔT was made (Sinyavsky, Pashkov, Gorovoy, Lugansky, and Shebanov, 1989; Xiao, Wang, Zhang, Peng, Zhu and Yang, 1998), most experimental studies were based on the Maxwell relations where the electric displacement D versus temperature T under different electric fields was characterized. ΔS and ΔT were deduced from Eqs. (6) and (7) (see below for details). For dielectric materials with low hysteresis loss and the measurement is in an ideal situation, results obtained from the two methods should be consistent with each other. However, as will be shown later that for the relaxor ferroelectric polymers, the ECE deduced from the

Maxwell relations can be very different from that measured directly and hence the Maxwell relations cannot be used for these materials in deducing ECE. In general, the Maxwell relations are valid only for thermodynamically equilibrium and ergodic systems.

In an ideal refrigeration cycle the working material (refrigerant) must absorb entropy (or heat) from the cooling load while in thermal contact with the load (isothermal entropy change ΔS). The material is then isolated from the load while the temperature is increased due to the application of external field (adiabatic temperature change ΔT). The material is then in thermal contact with the heat sink and entropy that was absorbed from the cooling load is rejected to the heat sink. The working material is then isolated from the heat sink and the temperature is reduced back as the field is reduced. The temperature of the refrigerant will be the same as the temperature of the cooling load when they are contacted. The whole process is repeated to further reduce the temperature of the load. Therefore, both the isothermal entropy change ΔS and the adiabatic temperature change ΔT are the key parameters for the ECE of a dielectric material for refrigeration (Wood and Potter, 1985; Kar-Narayan and Mathur, 2009).

2.2 Phenomenological theory of ECE

Phenomenological theory has been widely utilized to illustrate the macroscopic phenomena that occur in the polar materials, e.g. ferroelectric or ferromagnetic materials near their phase transition temperatures. The general form of the Gibbs free energy associated with the polarization can be expressed as a series expansion in terms of the electric displacement (Line and Glass, 1977)

$$G = \frac{1}{2}\alpha D^2 + \frac{1}{4}\xi D^4 + \frac{1}{6}\zeta D^6, \quad (8)$$

where $\alpha = \beta(T - T_0)$, and β , ξ and ζ are assumed to be temperature-independent phenomenological coefficients. From $\left(\frac{\partial G}{\partial T}\right)_D = -\Delta S$, one can obtain,

$$\Delta S = -\frac{1}{2}\beta D^2 \quad (9)$$

Then the adiabatic temperature change $\Delta T (=T\Delta S/c_E)$ can be obtained, i.e.

$$\Delta T = -\frac{1}{2c_E}\beta T D^2 \quad (10)$$

Based on Eqs. (9) and (10), the entropy will be reduced when the material changes to a polar state from a non-polar state when an external action, e.g. temperature, electric field or stress, is applied. The entropy change and temperature change are associated with the phenomenological coefficient β and electric displacement D , viz. proportional to β and D^2 . Both parameters will affect the ECE values of the materials. A material with large β and large D will generate large ECE entropy change and temperature change near the ferroelectric (F) - paraelectric (P) phase transition temperature.

2.3 ECE in several ferroelectric materials

Based on the literature reported values of β and D , the ECE values of various ferroelectric materials could be estimated. For instance, for BaTiO₃, $\beta = 6.7 \times 10^5 (\text{JmC}^{-2}\text{K}^{-1})$ and $D = 0.26$

C/m² (Jona and Shirane, 1993; Furukawa, 1984), ΔS will be approximately 3 J/(kgK). Using the specific heat $c_E = 4.07 \times 10^2$ J/(kgK) and $T_c = 107$ °C (Jona and Shirane, 1993; Akay, Alpay Mantese, and Rossetti Jr, 2007), results in a $\Delta T = 2.8$ °C. Similarly, for $\text{Pb}(\text{Zr}_x\text{Ti}_{1-x})\text{O}_3$ ($0.0 < x \leq 0.6$), $\beta = 1.88 \times 10^5$ and $D = 0.39$ C/m² (Amin, Cross, and Newnham, 1981; Amin, Newnham, and Cross, 1981), one will obtain $\Delta S = 1.8$ J/(kgK). Taking $T_c = 250$ °C, and $c_E = 3.4 \times 10^2$ J/(kgK) (PI Ceramic website, 2009), will result in $\Delta T = 2.7$ °C.

For ferroelectric polymers, e.g. P(VDF-TrFE), phenomenological theory predicts large ECE values. For example, P(VDF-TrFE) 65/35 mol% copolymer, with $\beta = 3.5 \times 10^7$ JmC⁻²K⁻¹ and $D = 0.08$ C/m² (Furukawa, 1984), will exhibit a $\Delta S = 62$ J/(kgK). Making use of its specific heat capacity $c_E = 1.4 \times 10^3$ J/(kgK) (Furukawa, Nakajima, and Takahashi, 2006) and Curie temperature $T_c = 102$ °C (Furukawa T, 1984), yields $\Delta T = 16.6$ °C. The large ΔS and ΔT values suggest that a large ECE may be achieved in ferroelectric P(VDF-TrFE) copolymers. Furthermore, relaxor ferroelectric polymers based on P(VDF-TrFE), such as P(VDF-TrFE-CFE) 59.2/33.6/7.2 mol% (CFE-chlorofluoroethylene) relaxor ferroelectric terpolymers also have potential to reach a large ECE because the β and D are still large.

It was found that β of ferroelectric ceramics ($\sim 10^5$) is about two orders of magnitude smaller than that of P(VDF-TrFE) ($\sim 10^7$). D however is only several times higher for ceramics, since $\Delta S \sim \beta D^2$, ΔS is still about one order of magnitude smaller than that of the P(VDF-TrFE) based polymers.

In addition, the heat of F-P phase transition can also be used to assess the ECE ($Q = T\Delta S$) in a ferroelectric material at temperatures above the F-P transition. For a very strong order-disorder ceramic system (an example of which is the ferroelectric ceramic triglycine sulphate, TGS), the heat of F-P phase transition is 2.0×10^3 J/kg (corresponding to an entropy change of $\Delta S \sim 6.1$ J/(kgK)). For BaTiO_3 , F-P heat is smaller 9.3×10^2 J/kg ($\Delta S \sim 2.3$ J/(kgK)) (Jona and Shirane, 1993). In other words, although ceramic materials may exhibit a higher adiabatic temperature change, their isothermal entropy change may not be very high. In contrast, ferroelectric polymers offer higher heat of transition in a F-P transition. For instance, P(VDF-TrFE) 68/32 mol% copolymer shows a heat of F-P transition of more than 2.1×10^4 J/kg (or $\Delta S \sim 56.0$ J/(kgK)) (Neese, Chu, Lu, Wang, Furman and Zhang, 2008). This is approximately 10 times larger than its inorganic counterparts.

3. Investigations on ECE in polar materials

3.1 ECE studies in ferroelectric ceramics and single crystals

The history of ECE study may be traced back to as early as 1930s. In 1930, Kobeko and Kurtschatov did a first investigation on ECE in Rochelle salt (Kobeko and Kurtschatov, 1930), however they did not report any numerical values. In 1963, Wiseman and Kuebler redid their measurements (Wiseman and Kuebler, 1963), obtaining $\Delta T = 0.0036$ °C in an electric field of 1.4 kV/cm at 22.2 °C. In their study, the Maxwell relation was used to derive $\Delta T (\Delta T = -\frac{T}{c_E} \frac{\partial \alpha}{\partial T} D \Delta D)$, where $\alpha = 1/\epsilon$ as defined in Eq. (8) and ϵ is the permittivity). The isothermal entropy change was 28.0 J/m³K (1.56×10^{-2} J/(kgK)).

Other studies on inorganic materials used KH_2PO_4 crystal, and SrTiO_3 , $\text{Pb}(\text{Sc}_{0.5}\text{Ta}_{0.5})\text{O}_3$, and $\text{Pb}_{0.98}\text{Nb}_{0.02}(\text{Zr}_{0.75}\text{Sn}_{0.20}\text{Ti}_{0.05})_{0.98}\text{O}_3$ ceramics. For KH_2PO_4 crystal, Maxwell relation was used in the form of $\Delta T = -(T/c_E) \left(\frac{\partial D/\partial T}{\partial D/\partial E} \right) dD$ to obtain $\Delta T = 1$ °C for a 11 kV/cm electric field and an entropy change of 2.31×10^3 J/m³K (or 0.99 J/(kgK)) (Baumgartner, 1950). For SrTiO_3 , ΔT

=1 °C and $\Delta S=34.63 \text{ J/m}^3\text{K}$ ($6.75 \times 10^{-3} \text{ J/(kgK)}$) under 5.42 kV/cm electric field at 4 K from Eq. (7) (Lawless and Morrow, 1977). For $\text{Pb}(\text{Sc}_{0.5}\text{Ta}_{0.5})\text{O}_3$, a $\Delta T=1.5 \text{ °C}$ and ΔS of $1.55 \times 10^4 \text{ J/m}^3\text{K}$ (1.76 J/(kgK)) were measured directly for a sample under 25 kV/cm field at 25 °C (Sinyavsky and Brodyansky, 1992). For $\text{Pb}_{0.98}\text{Nb}_{0.02}(\text{Zr}_{0.75}\text{Sn}_{0.20}\text{Ti}_{0.05})_{0.98}\text{O}_3$, $\Delta T=2.5 \text{ °C}$ and $\Delta S=1.73 \times 10^4 \text{ J/m}^3\text{K}$ (2.88 J/(kgK)) at 30 kV/cm and 161 °C deduced from Eq. (7) (Tuttle and Payne, 1981).

A direct ECE measurement was carried out for $(1-x)\text{Pb}(\text{Mg}_{1/3}\text{Nb}_{2/3})\text{O}_3-x\text{PbTiO}_3$ ($x=0.08, 0.10, 0.25$) ceramics near room temperature using a thermocouple when a dc electric field was applied (Xiao, Wang, Zhang, Peng, Zhu and Yang, 1998). A temperature change of 1.4 °C was observed for $x=0.08$ although at high temperatures (as x increased), this change was reduced. This high ECE can be accounted for by considering the electric field-induced first-order phase transition from the mean cubic phase to 3m phase.

These results indicate that the ECE in ceramic and single crystal materials are relatively small, viz. $\Delta T < 2.5 \text{ °C}$, and $\Delta S < 2.9 \text{ J/(kgK)}$, mainly because the breakdown field is low, using applied electric fields that are less than 3 MV/m. Defects existing in bulk materials cause early breakdown and empirically the breakdown electric field was inversely proportional to the material's thickness. For piezoelectric ceramics, the breakdown field (in kV/cm) is related to the thickness (in cm) via the relationship, $E_b=27.2t^{-0.39}$, indicating that thin films are more appropriate for an ECE study. Additionally, the breakdown field of dielectric polymers can be several orders of magnitude higher than ceramics, suggesting polar-polymers are good candidates for ECE investigations.

3.2 ECE in ferroelectric and antiferroelectric thin films

In 2006, Mischenko et al. investigated ECE in sol-gel derived antiferroelectric $\text{PbZr}_{0.95}\text{Ti}_{0.05}\text{O}_3$ thin films near the F - P transition temperature. In their study, films with 350 nm thickness were used to allow for electric fields as high as 48 MV/m. An adiabatic temperature change of 12 °C was obtained (as deduced from Eq. (7)) at 226 °C, slightly above the phase transition temperature (222°C) (Mischenko, Zhang, Scott, Whatmore and Mathur, 2006). Both the high electric field and the high operation temperature near phase transition contribute to the large ΔT ($=T\Delta S/C_E$). On the other hand, its isothermal entropy change is estimated to be 8 J/(kgK), which is not high compared with magnetic alloys exhibiting giant magnetocaloric effect (MCE) near room temperature, where $\Delta S \geq 30 \text{ J/(kgK)}$ was observed (Provenzano, Shapiro and Shull, 2004). As stated previously, for high performance refrigerants, a large ΔS is necessary (Wood and Potter, 1985).

To reduce the operational temperature for large ECE in ceramic thin films, Correia et al. successfully fabricated $\text{PbMg}_{1/3}\text{Nb}_{2/3}\text{O}_3\text{-PbTiO}_3$ thin films with perovskite structure using $\text{PbZr}_{0.8}\text{Ti}_{0.2}\text{O}_3$ seed layer on Pt/Ti/TiO₂/SiO₂/Si substrates (Correia, Young, Whatmore, Scott, Mathur and Zhang, 2009). A temperature change of $\Delta T=9 \text{ K}$ was achieved at 25 °C. An entropy change of 9.7 J/(kgK) can be deduced. A significant difference for ferroelectric thin films is that the largest ΔT occurs at 25 °C, near the depolarization temperature (18 °C), not above the permittivity peak temperature. The large ECE only happens at field heating. Transitions for stable and metastable polar nanoregions (PNR) to nonpolar regions are accounted for by observed phenomena. Interactions of PNRs are similar to that between the dipoles in a glass. The field-induced phase transition has been observed in PMN-PT single crystals (Lu, Xu and Chen, 2005; Ye and Schmid, 1993). Thermal history has a critical impact on the field-induced phase transition. Relaxor ferroelectrics are of great interest due to their

phase transition temperatures being near or at room temperature. The field induced phase transition may produce larger polarization, e.g. induced polarization, $\langle P_d \rangle$, which can lead to larger dP/dT as well as large ΔS and ΔT .

For thin film, the substrate must be taken into account as it may exert stresses on the thin film due to the misfit of the lattices and electromechanical coupling from the strain changes under electric field. The free energy of thin film is subject to lateral clamping and may be expressed as (Akay, Alpay Mantese, and Rossetti Jr, 2007)

$$G_{film} = G_0 + \tilde{\alpha}D^2 + \tilde{\xi}D^4 + \tilde{\zeta}P^6 - EP + G_{strain}, \quad (11)$$

where

$$\tilde{\alpha} = \alpha - 2u_m Q_{12} \tilde{C} \quad (12)$$

and

$$\tilde{\beta} = \beta + Q_{12}^2 \tilde{C} \quad (13)$$

are the modified phenomenological coefficients, $G_{strain} = u_m^2 \tilde{C}$ is the polarization-free strain energy, $\tilde{C} = C_{11} + C_{12} - 2C_{12}^2 / C_{11}$, C_{ij} are the elastic constants at constant polarization, Q_{ij} are the cubic electrostrictive coefficients, and u_m is the in-plane misfit strain. The phase transition temperature varies linearly with the lattice misfit strain via Eq. (12) while the two-dimensional clamping is illustrated by Eq. (13). The excess entropy S_E^{XS} and specific heat ΔC_E of the ferroelectric phase transition follow the form (Akay, Alpay Mantese, and Rossetti Jr, 2007),

$$S_E^{XS}(T, E) = -T \left(\frac{\partial G(D)}{\partial T} \right)_E, \quad (14)$$

$$\Delta C_E(T, E) = -T \left(\frac{\partial^2 G(D)}{\partial T^2} \right)_E. \quad (15)$$

It was found that for BaTiO₃ (BTO) thin film deposited on substrate, perfect lateral clamping of BTO will transform the discontinuous phase transition (1st order phase transition) into a continuous one. Accordingly the polarization and the specific heat capacity will be reduced near the phase transition temperature. On the other hand, based on Eqs. (12) and (13), adjustment of misfit strain in epitaxial ferroelectric thin films may vary the magnitude and temperature dependencies of their ECE properties.

4. Large ECE in ferroelectric polymer films

4.1 Direct method to measure ECE

Although most of the ECE studies rely on Maxwell relation (indirect method) to deduce the ECE of a material, it is always desirable to directly measure ECE in a dielectrics as refrigerants in cooling devices, i.e., to directly measure the isothermal entropy change ΔS and adiabatic temperature change ΔT induced by a change in the applied field (direct

method). In our study, both the indirect method and direct method were employed to characterize the ECE in polymer films. The direct comparison of the results from two methods can also shed light on how reliable the indirect method is in deducing the ECE from a ferroelectric material.

There are several methods that have been used in measuring the magnetocaloric effect (MCE) in terms of measuring the isothermal entropy change and adiabatic temperature change, such as thermocouple (Dinesen, Linderroth and Morup, 2002; Lin, Xu and Zhang, 2004; Spichkin, Derkachb, Tishin, Kuz'min, Chernyshov, Gschneidner Jr, and Pecharsky, 2007), thermometer (Gopal, Chahine and Bose, 1997), and calorimeter (Tocado, Palacios and Burriel, 2005; Pecharsky, Moorman and Gschneidner, Jr, 1997).

Here, a high resolution calorimeter was used to measure the sample temperature variation due to ECE when an external electric field was applied (Yao, Ema and Garland, 1998). The temperature signal was measured by a small bead thermistor. A step-like pulse was generated by a functional generator to change the applied electric field in the film, and the width of the pulse was chosen so that the sample can reach thermal equilibrium with surrounding bath. Due to the fast electric as well as thermal response (ECE) of the polymer films (in the order of tens of milliseconds (Furukawa, 1989), a simple zero-dimensional model to describe the thermal process can be applied with sufficient accuracy. In a relaxation mode, the temperature $T(t)$ of the whole sample system can be measured, which has an exponential relationship with time, i.e.

$$T(t) = T_{bath} + \Delta T e^{-t/\tau}, \quad (16)$$

where T_{bath} is the initial temperature of the film, ΔT the temperature change of the polymer film. The total temperature change ΔT_{EC} of the whole sample system was measured, which can be expressed as $\Delta T_{EC} = \Delta T \sum C_p^i / C_p^{EC}$. Here, C_p^i represents the heat capacity of each subsystem, C_p^{EC} is the heat capacity of the polymer film covered with electrode. ΔT_{EC} was measured as a function of temperature at constant electric field and as a function of electric field at constant temperature. ΔS can be determined from $T\Delta S = C_p^i \Delta T$.

4.2 ECE in the normal ferroelectric P(VDF-TrFE) 55/45 mol% copolymer

4.2.1 Experimental results of ECE

As indicated in Section 2, the ferroelectric copolymer may produce large ECE near its phase transition temperature. P(VDF-TrFE) 55/45 mol% was chosen because its F-P phase transition is of second-order (continuous), thus avoiding the thermal hysteresis effect associated with the first-order phase transition. In addition, among all available P(VDF-TrFE) copolymers, this composition exhibits the lowest F-P phase transition temperature ($\sim 70^\circ\text{C}$), which is favorable for refrigeration near room temperature.

Polymer films used for the indirect ECE measurement were prepared using a spin-casting method on metalized glass substrates. The film thickness for this study was in the range of $0.4\ \mu\text{m}$ to $1\ \mu\text{m}$. The free-standing films for the direct ECE measurement were fabricated using a solution cast method and the film thickness is in the range of $4\ \mu\text{m}$ to $6\ \mu\text{m}$. Figure 2 shows the permittivity as a function of temperature for P(VDF-TrFE) 55/45 mol% copolymers measured at 1 kHz. It can be seen that the thermal hysteresis between the heating and cooling runs is pretty small ($\sim 1^\circ\text{C}$). The remanent polarization as a function of

temperature shown in Fig. 3 further indicates a second-order phase transition occurred in the material. The phase transition temperature is about 70 °C, and the glass transition temperature is about -20 °C. At temperature higher than 100 °C, the loss tangent rises sharply, which is associated with the thermally activated conduction.

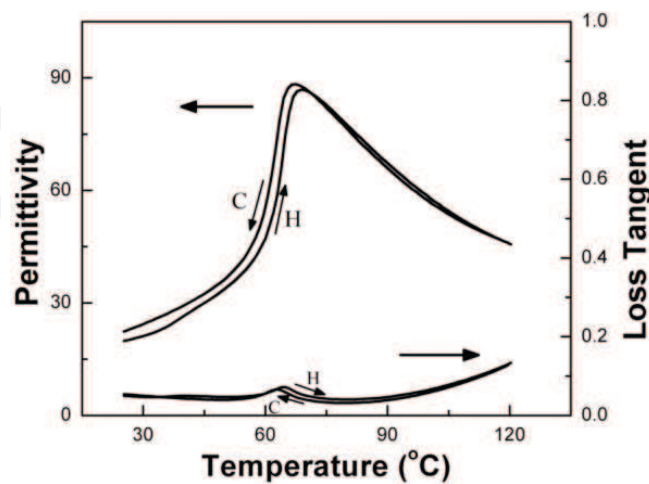


Fig. 2. Permittivity as a function of temperature for P(VDF-TrFE) 55/45 mol% copolymers.

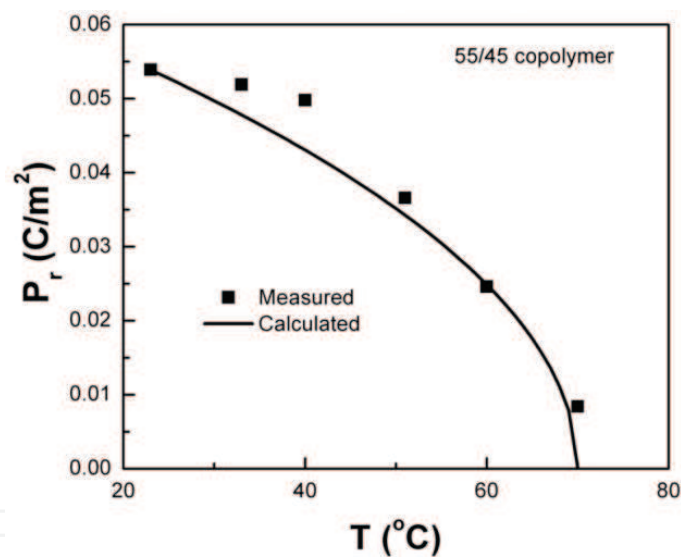


Fig. 3. Remanent polarization as a function of temperature for P(VDF-TrFE) 55/45 mol% copolymers.

Figure 4 shows the electric displacement as a function of electric field measured at various temperatures. At temperatures below the transition temperature, the polymer film is in a ferroelectric state, the normal hysteresis loop is observed while at higher temperatures, the loop becomes slimed, remanent polarization diminishes, and saturation polarization still exists. Hence the electric displacement as a function of electric field at different temperatures can be procured, which is presented in Fig. 5 (Neese, 2009). One can see that the electric displacement monotonically decreases with temperature above the phase transition. The Maxwell relations were used to calculate the isothermal entropy change and adiabatic temperature change as a function of ambient temperature. The results deduced are presented in Figs. 6 and 7.

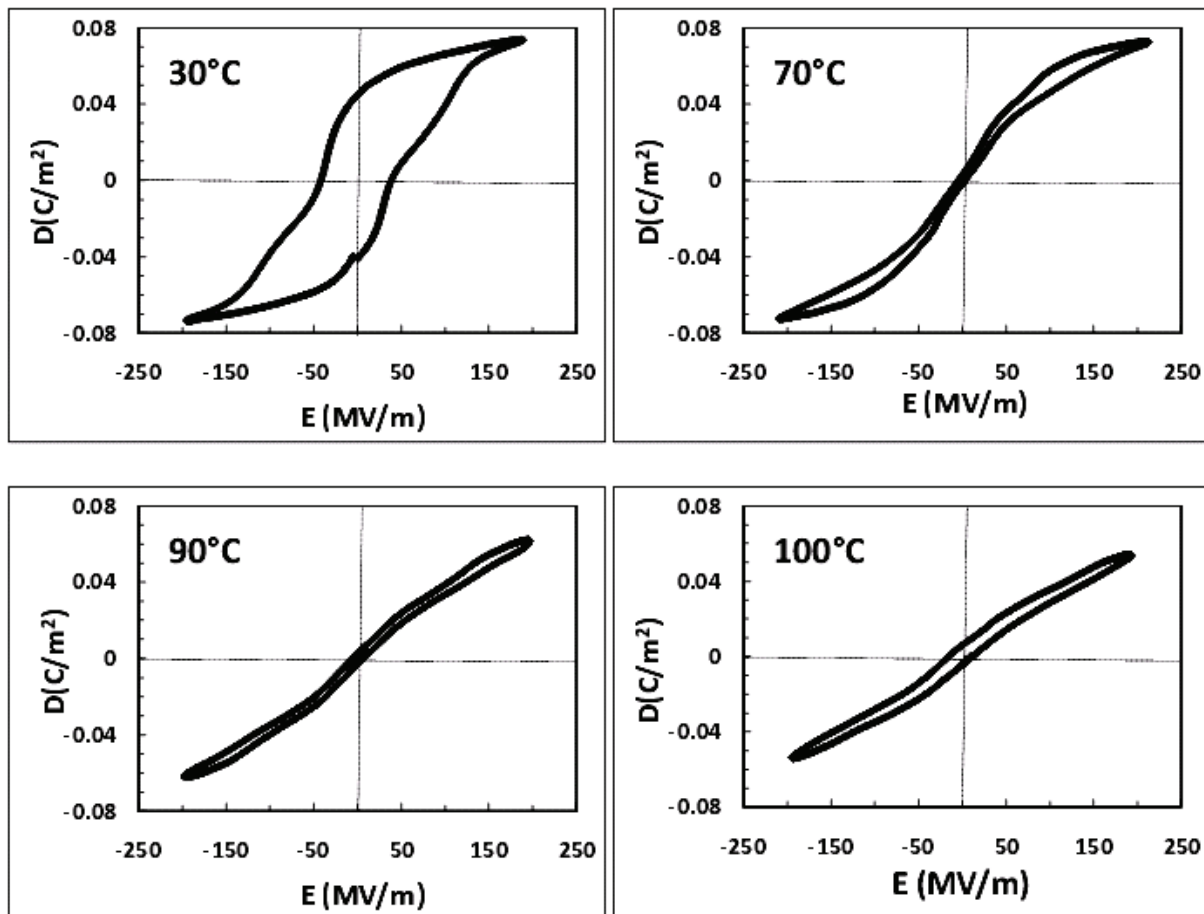


Fig. 4. Electric displacement – electric field hysteresis loops at temperature below and above the phase transition.

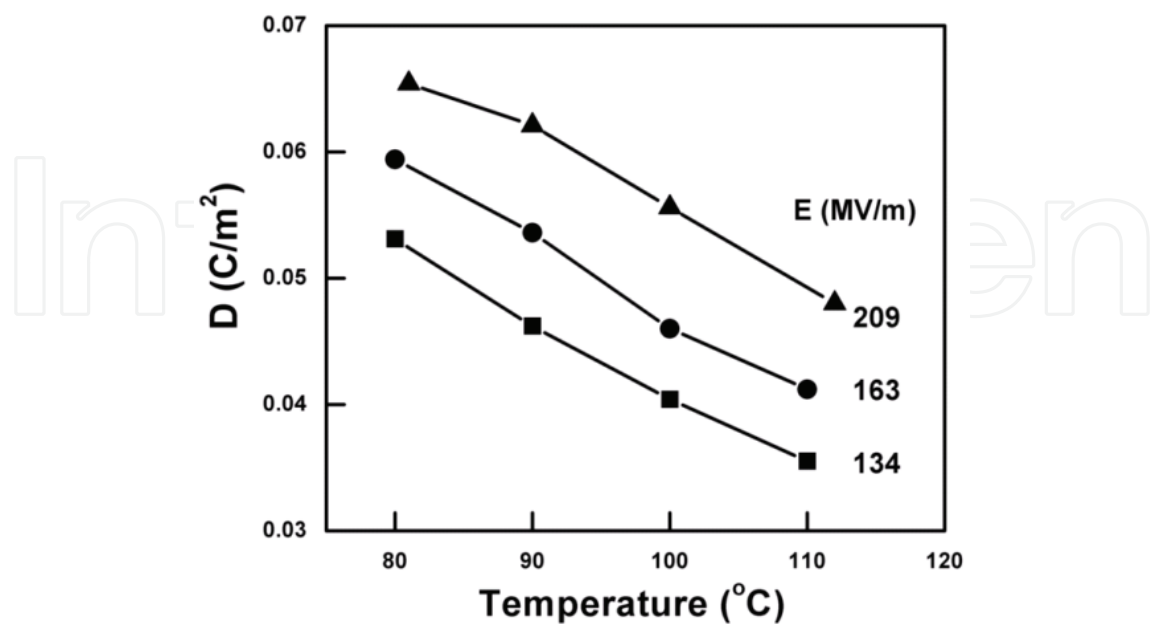


Fig. 5. Electric displacement as a function of temperature at different electric fields for P(VDF-TrFE) 55/45 mol% copolymers.

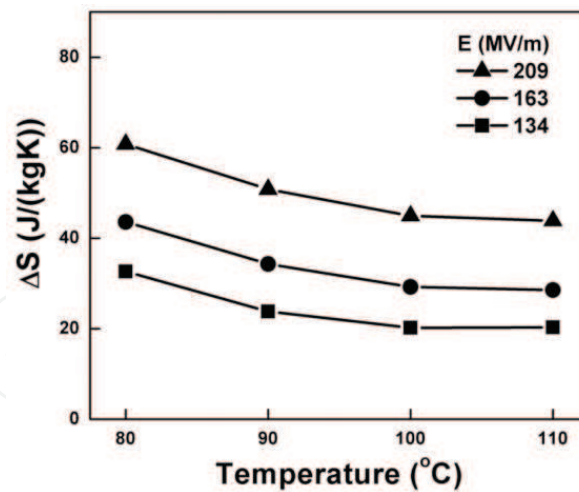


Fig. 6. Isothermal entropy changes as a function of ambient temperature at different electric fields.

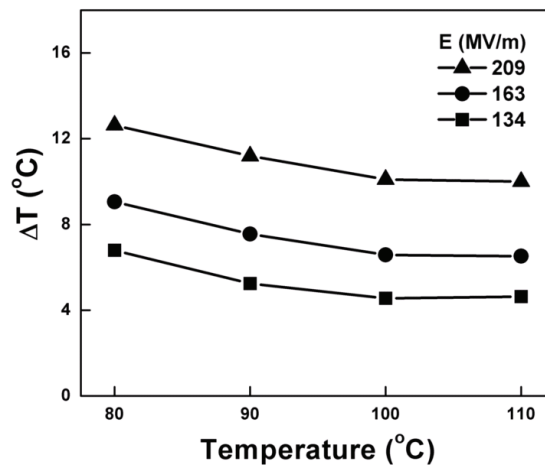


Fig. 7. Adiabatic temperature changes as a function of ambient temperature at different electric fields.

Present in Fig. 8 is the directly measured ΔS and ΔT as a function of temperature measured under several electric fields for the unstretched P(VDF-TrFE) 55/45 mol% copolymer. As can be seen, the ECE effect reaches maximum at the temperature of FE-PE transition. A comparison between the directly measured and deduced ECE indicates that within the experimental error, the ECE deduced from the Maxwell relation is consistent with that directly measured. Therefore, for a ferroelectric material at temperatures above F-P transition, Maxwell relation can be used to deduce ECE.

4.2.2 Phenomenological calculations on ECE

It is well established by many studies (see Fig. 2) that the F-P phase transition of P(VDF-TrFE) 55/45 copolymer is of second-order. For the copolymer with 2nd order phase transition, free energy associated with polarization can be written as

$$G = G_0 + \frac{1}{2}\beta(T - T_c)P^2 + \frac{1}{4}\xi P^4 - EP \quad (17)$$

where G_0 is the free energy of the material not associated with polarization, β and ξ are phenomenological coefficients, that are assumed temperature independent. T_c is the Curie temperature, E the electric field, and P the polarization.

Differentiating G with respect to P yields the relationship between E and P ,

$$E = \beta(T - T_c)P + \xi P^3. \quad (18)$$

When $E=0$ and at $T < T_c$,

$$P^2 = \beta(T - T_c) / \xi. \quad (19)$$

Further differentiating the Eq. (18) yields the reciprocal permittivity,

$$\frac{1}{\epsilon} = \beta(T - T_c) + 3\xi P^2 \quad (T < T_c). \quad (20)$$

$$\frac{1}{\epsilon} = \beta(T - T_c) \quad (T \geq T_c). \quad (21)$$

Using Eqs. (19) and (21), the permittivity versus temperature (Fig. 2), and the polarization versus temperature relationships (Fig. 3), β and ξ can be obtained. Their values are, $\beta = 2.4 \times 10^7$ ($\text{JmC}^{-2}\text{K}^{-1}$), and $\xi = 3.9 \times 10^{11}$ (Jm^5C^{-4}).

Now Eq. (18) can be used to derive the polarization as a function of temperature under different DC bias fields. Before doing the calculation, it should be noted that the F-P transition temperature is a function of DC bias field. This relationship was obtained by directly measuring the permittivity as a function of temperature in different DC bias fields. The results are shown in Fig. 9.

However, the dielectric measurement becomes extremely difficult when $E_{DC} > 100$ MV/m. Hence, the relationship of $\Delta T_c - E^{2/3}$ (Lines and Glass, 1977) was fitted and extrapolated to obtain T_c at $E > 100$ MV/m.

The calculated polarization versus temperature relationships under different DC biases are shown in Fig. 10. Based on the D-T data, the ΔS and ΔT can be calculated via Eqs. (6) and (7). Results are shown in Figs. 11 and 12.

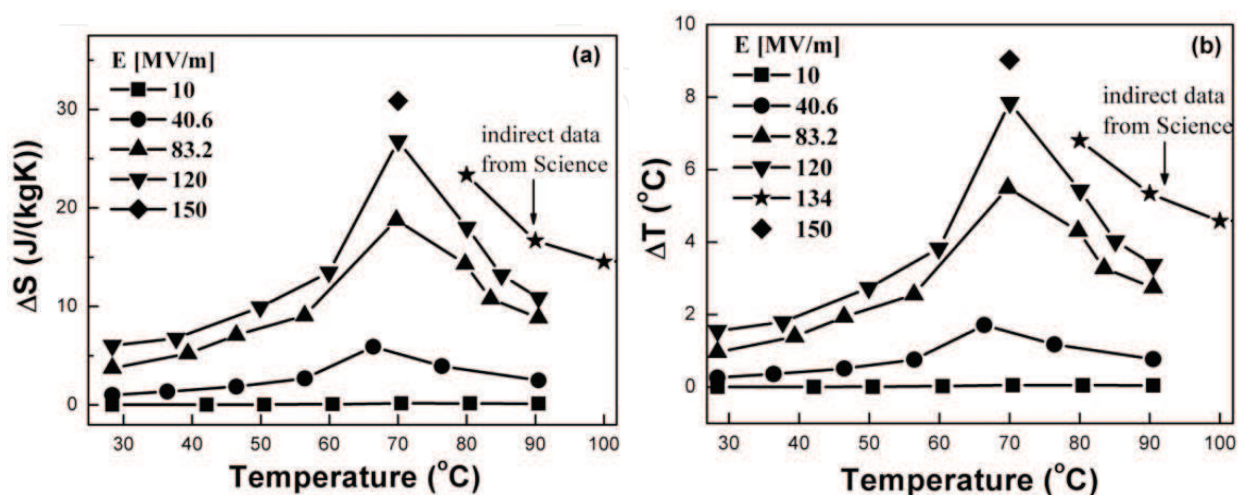


Fig. 8. Directly measured ΔS (a) and ΔT (b) as a function of temperature under several electric fields for unstretched P(VDF-TrFE) 55/45 mol% copolymers.

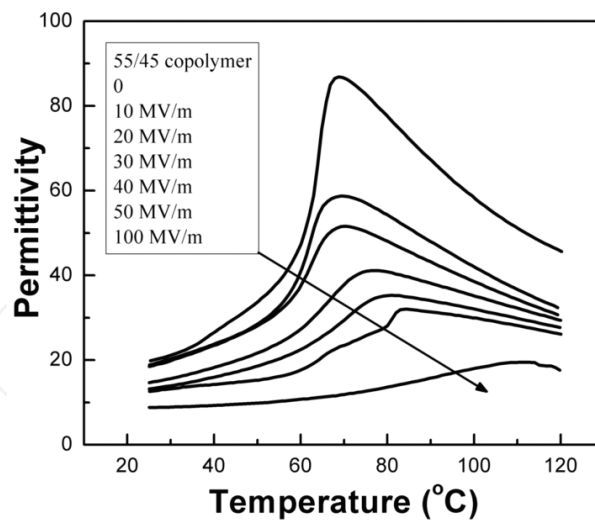


Fig. 9. Permittivity as a function of temperature at 1 kHz in various DC bias fields for 55/45 copolymer.

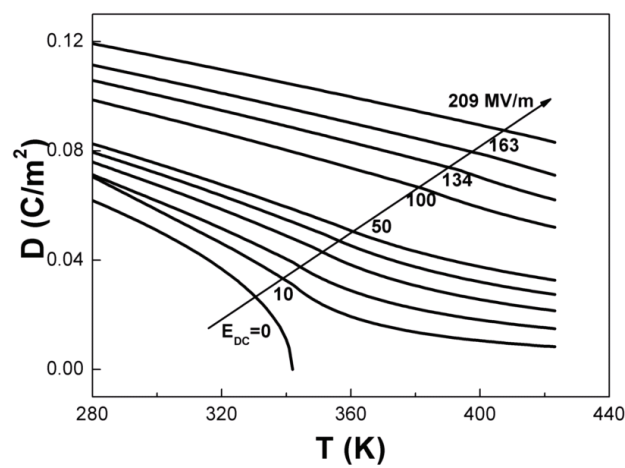


Fig. 10. Polarization versus temperature relationships with various DC biases for 55/45 copolymer.

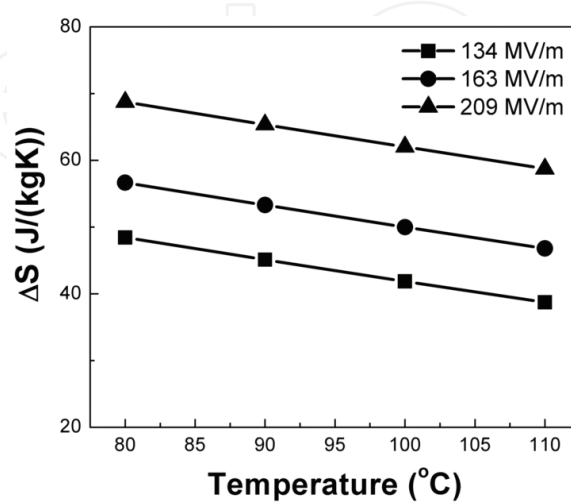


Fig. 11. ECE entropy changes versus temperature for 55/45 copolymer.

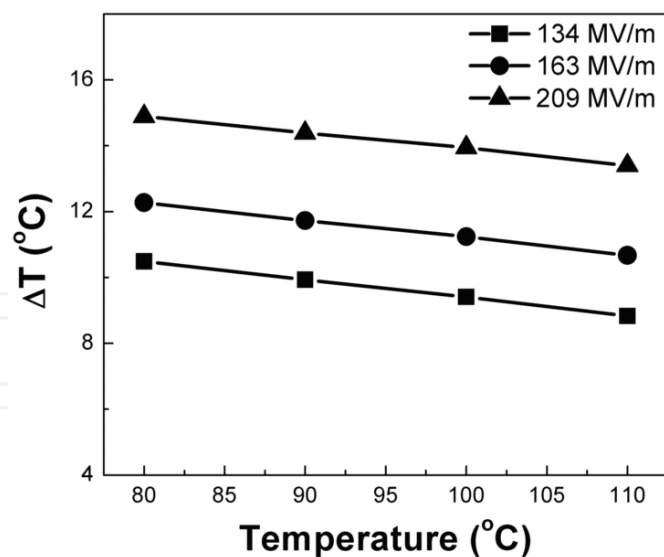


Fig. 12. ECE temperature changes versus temperature for 55/45 copolymer.

Phenomenological calculation indicates that, there is a giant ECE exhibited by P(VDF-TrFE) 55/45 copolymers. The ΔS and ΔT can reach 70 J/(kgK) and 15 °C respectively near the phase transition temperature ~ 70 °C. It can also be seen that ΔS has a linear relationship with D^2 (or P^2), the slope is $1/2\beta$.

4.3 ECE in the relaxor ferroelectric P(VDF-TrFE-CFE) terpolymers

Both the pure relaxor ferroelectric P(VDF-TrFE-CFE) 59.2/33.6/7.2 mol% terpolymer and blends with 5% and 10% of P(VDF-CTFE) copolymer were studied. For the P(VDF-TrFE-CFE) relaxor terpolymer, it was observed that blending it with a small amount of P(VDF-CTFE) 91/9 mol% copolymer [CTFE: chlorotrifluoroethylene] can result in a large increase in the elastic modulus, especially at temperatures above the room temperature, which does not affect the polarization level very much. Such an increase in the elastic modulus

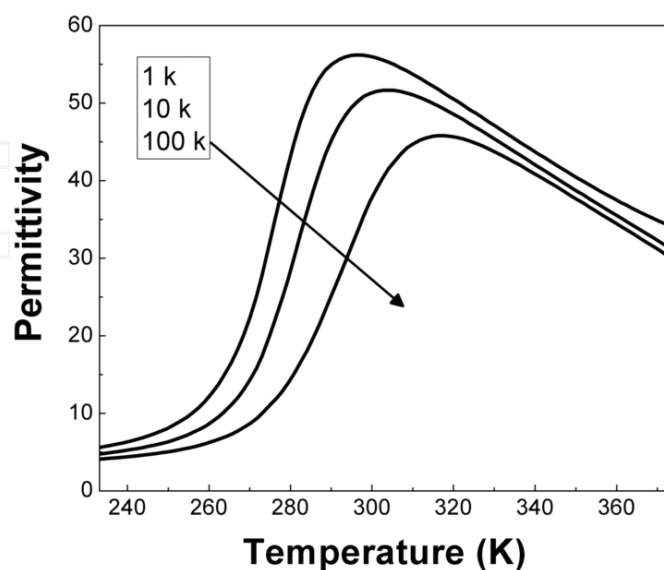


Fig. 13. Permittivity as a function of temperature at 1, 10 and 100 kHz for 59.2/33.6/7.2 mol% terpolymer.

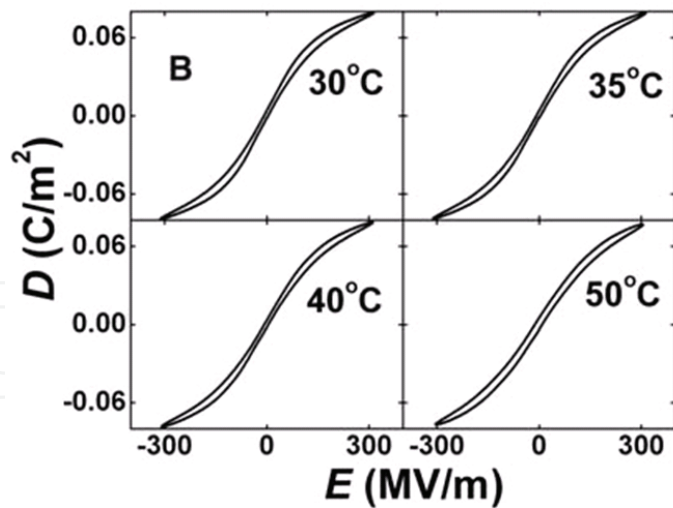


Fig. 14. Electric displacement – electric field hysteresis loops at temperature above the phase transition for 59.2/33.6/7.2 mol% terpolymers.

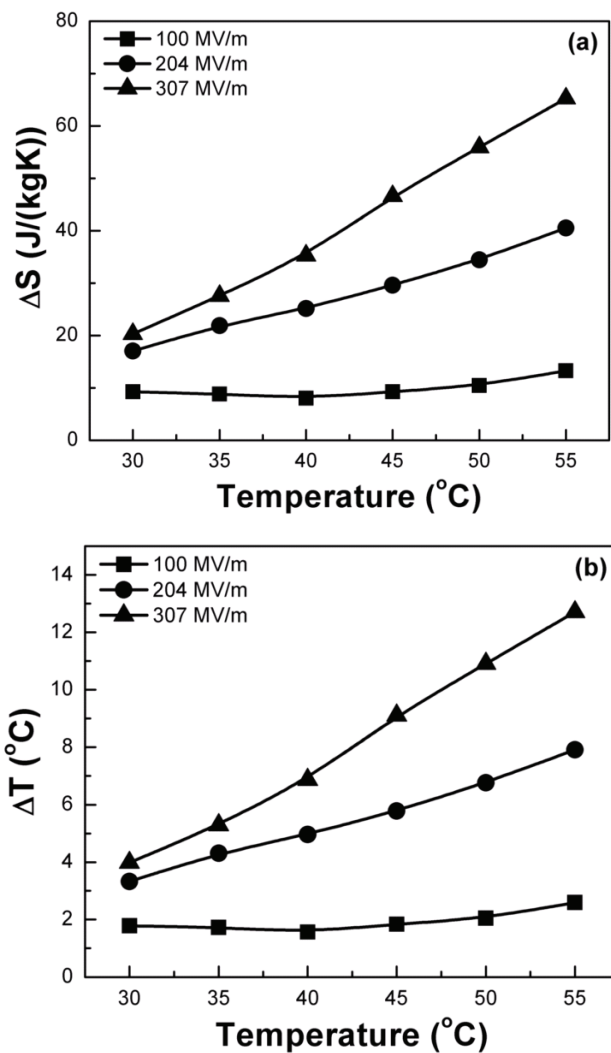


Fig. 15. ECE entropy changes (a) and temperature change (b) versus temperature deduced from Maxwell relation for 59.2/33.6/7.2 mol% terpolymer.

improves the dielectric strength of the blend polymer films and allows the direct measurement of ECE to be carried out to higher fields (>100 MV/m).

Present in Fig. 13 is the dielectric constant data for the terpolymer. The D-E loops for the P(VDF-TrFE-CFE) 59.2/33.6/7.2 mol% terpolymer are presented in Fig. 14, from which ΔS and ΔT are deduced from the Maxwell relation as shown in Fig. 15 (a) and 15 (b), respectively. The results show that the terpolymer has a weak ECE at room temperature and increases with temperature. At 55 °C which is the highest temperature measured, a $\Delta S=55$ J/(kgK) and $\Delta T=12$ °C under the field of 307 MV/m are deduced from the Maxwell relation.

The ECE from the direct measurement is presented in Fig. 16, which is for the 59.2/33.6/7.2 mol% terpolymer. The data show quite different behavior compared with Fig. 15. First of all, the directly measured ECE from the relaxor terpolymer is much larger than that deduced from the Maxwell relation. Moreover, the directly measured ECE shows much weak temperature dependence at $E < 70$ MV/m.

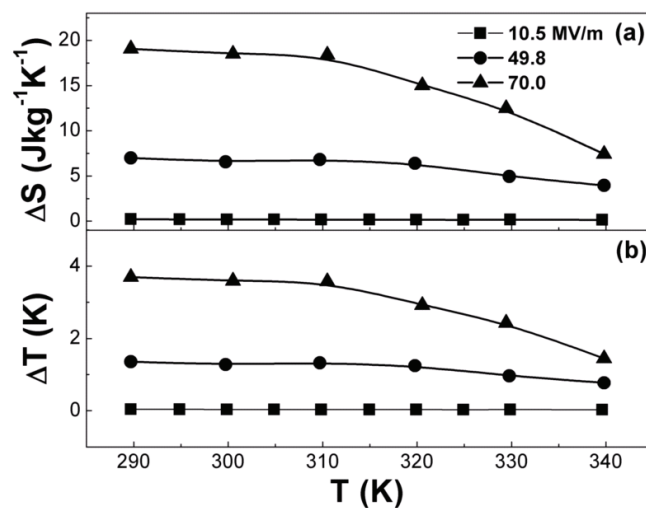


Fig. 16. Directly measured entropy changes (a) and temperature change (b) versus temperature for 59.2/33.6/7.2 mol% terpolymer .

The results indicate that the Maxwell relation is not suitable for ECE characterization for the relaxor ferroelectric polymers even at temperatures above the broad dielectric constant maximum. This is likely caused by the non-ergodic behaviour of relaxor ferroelectric polymers even at temperatures above the dielectric constant maximum while the Maxwell relations are valid only for thermodynamically equilibrium systems (ergodic systems)

We also note that a recent report of ECE deduced from the Maxwell relation on a P(VDF-TrFE-CFE) relaxor ferroelectric terpolymer by Liu et al. (Liu et al. 2010) shows very irregular field dependence of ECE measured at temperatures below 320 K where ECE in fact decreases with field, which is apparently not correct. These results all indicate that the Maxwell relation cannot be used to deduce ECE for the relaxor ferroelectric polymers, or even the relaxor ferroelectric materials in general, even at temperatures far above the freezing transition and the broad dielectric constant peak temperature.

5. Conclusions

General considerations for polar materials to achieve larger ECE were presented based on the phenomenological theory analysis. It is shown that in order to realize large ECE, a

dielectric material with a large polarization P as well as large phenomenological coefficient β is required. It is further shown that both the phenomenological consideration and experimental data on heat of ferroelectric-paraelectric transition suggest that ferroelectric P(VDF-TrFE) based polymers have potential to achieve giant ECE. Indeed, experimental results show that the normal ferroelectric P(VDF-TrFE) 55/45 mol% copolymers exhibit a large ECE, i.e., an adiabatic temperature change over 12 °C and an isothermal entropy change over 50 J/(kgK) were obtained. The experimental results also indicate that for the normal ferroelectric materials, the ECE deduced from the Maxwell relation is consistent with that directly measured.

The experimental results on ECE in the relaxor ferroelectric P(VDF-TrFE-CFE) terpolymer were also presented which reveal a very large ECE at ambient condition in the relaxor terpolymers. In contrast to the normal ferroelectric polymers, the ECE deduced from the Maxwell relation for the relaxor terpolymers significantly deviates from that directly measured. The results indicate that the Maxwell relation is not suitable for ECE characterization for the relaxor ferroelectric polymers even at temperatures above the broad dielectric constant maximum. This is likely caused by the non-ergodic behaviour of relaxor ferroelectric polymers even at temperatures above the dielectric constant maximum while the Maxwell relations are valid only for thermodynamically equilibrium systems (ergodic systems).

As a final point, one interesting question to ask when searching for electrocaloric materials to achieve giant ECE at ambient temperature is how to design dielectric materials to significantly enhance the entropy in the polar-disordered state since ECE is directly related to the entropy difference between the polar-disordered and ordered states in a dielectric material, in other words, how to design a ferroelectric material to increase β while maintaining large D in Eqs. (9) and (10). This is certainly an interesting area of research. The successful outcome will have significant impact on the society, in terms of efficient energy use for refrigeration, new and compact cooling devices which are more environmentally friendly.

6. Acknowledgements

The works at Penn State University was supported by the US Department of Energy, Division of Materials Sciences, under Grant No. DE-FG02-07ER46410. The work at Jozef Stefan Institute was supported by the Slovenian Research Agency. The authors thank B. Neese, B. Chu, Y. Wang, E. Furman, Xinyu Li, and Lee J. Gorny for their contributions to the works presented in this chapter.

7. References

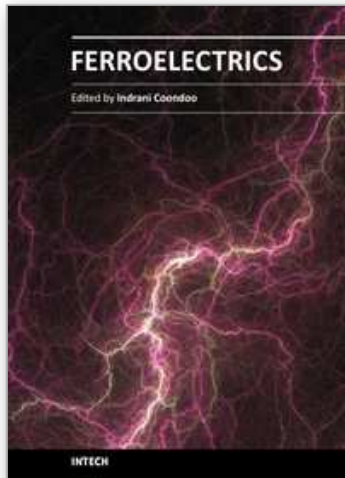
- Akcay, G.; Alpay, S. P.; Mantese, J. V. & Rossetti Jr., G. A. (2007). Magnitude of the intrinsic electrocaloric effect in ferroelectric perovskite thin films at high electric fields. *Appl Phys Lett*, 90 (25) (JUN, 2007), 252909/1-3. ISSN: 0003-6951.
- Amin, A.; Cross, L. E. & Newnham, R. E. (1981). Calorimetric and phenomenological studies of the PbZrO₃-PbTiO₃ system. *Ferroelectrics*, 37 (1-4) (1981), 647-650. ISSN: 0015-0193.
- Amin, A.; Newnham, R. E.; Cross, L. E. & Cox, D. E. (1981). Phenomenological and structural study of a low-temperature phase-transition in the PbZrO₃-PbTiO₃ system. *J. Solid State Chem*, 37 (2) (1981), 248-255. ISSN: 0022-4596.

- Baumgartner, H. (1950). Elektrische sättigungserscheinungen und elektrokalischer effect von kaliumphosphat KH_2PO_4 . *Helv Phys Acta*, 23 (6-7) (1950), 651-696. ISSN: 0018-0238.
- Correia, T. M.; Young, J. S.; Whatmore, R. W.; Scott, J. F.; Mathur, N. D. & Zhang, Q. (2009). Investigation of the electrocaloric effect in a $\text{PbMg}_{1/3}\text{Nb}_{2/3}\text{O}_3$ - PbTiO_3 relaxor thin film. *Appl Phys Lett*, 95 (18) (NOV, 2009), 182904/1-3. ISSN: 0003-6951.
- Dinesen, A. R.; Linderoth, S. & Mørup, S. (2002). Direct and indirect measurement of the magnetocaloric effect in a $\text{La}_{0.6}\text{Ca}_{0.4}\text{MnO}_3$ ceramic perovskite. *J. Magn Magn Mater*, 253 (1-2) (DEC, 2002), 28-34. ISSN: 0304-8853.
- Epstein, R. & Malloy, K. J. (2009). Electrocaloric devices based on thin-film heat switches. *J Appl Phys*, 106 (6) (SEP, 2009), 064509/1-7. ISSN: 0021-8979.
- Furukawa, T. (1984). Phenomenological aspect of a ferroelectric vinylidene fluoride / trifluoroethylene copolymer. *Ferroelectrics*, 57 (1-4) (1984), 63-72. ISSN: 0015-0193.
- Furukawa, T. (1989). Piezoelectricity and pyroelectricity in polymers. *IEEE Trans Electr Ins*, 24 (3) (JUN, 1989), 375-394. ISSN: 0018-9367.
- Furukawa, T.; Nakajima, T. & Takahashi, Y. (2006). Factors governing ferroelectric switching characteristics of thin VDF/TrFE copolymer films. *IEEE Trans Diel Electr Ins*, 13 (5) (OCT, 2006), 1120-1131. ISSN: 1070-9878.
- Gopal, B. R.; Chahine, R. & Bose, T. K. (1997). A sample translatory type insert for automated magnetocaloric effect measurements. *Rev Sci Instrum*, 68 (4) (APR, 1997), 1818-1822. ISSN: 0034-6748.
- Gschneidner Jr., K. A.; Pecharsky, V. K. & Tsokol, A. O. (2005). Recent developments in magnetocaloric materials. *Rep Prog Phys*, 68, 1479-1539. ISSN: 0034-4885.
- Jona, F. & Shirane, G. (1993). *Ferroelectric Crystals*. Dover Publications, Inc. ISBN: 0486673863, 9780486673868. New York.
- Kar-Narayan, S. & Mathur, N. (2009). Predicted cooling powers for multilayer capacitors based on various electrocaloric and electrode materials. *Appl. Phys. Lett.* 95, 242903/1-3.
- Kobeko, Von P. & Kurtschatov, J. (1930). Dielektrische eigenschaften der seignettesalzkrystalle', *Z Phys*, 66, 192-205. ISSN: 0340-2347.
- Kucherov, Y. R. (1997). 'Piezo-pyroelectric energy converter and method', US Patent, US 5644184.
- Lang, S. B. (1976). Cryogenic refrigeration utilizing electrocaloric effect in pyroelectric lithium sulfate monohydrate. *Ferroelectrics*, 11 (3-4) (1976), 519-523. ISSN: 0015-0193.
- Lawless, W. N. & Morrow, A. J. (1977). Specific heat and electrocaloric properties of a SrTiO_3 ceramic at low temperatures. *Ferroelectrics*, 15 (3-4) (1977), 159-165. ISSN: 0015-0193.
- Lin, G. C.; Xu, C. D. & Zhang, J. X. (2004). Magnetocaloric effect in $\text{La}_{0.80-x}\text{Ca}_{0.20}\text{Sr}_x\text{MnO}_3$ ($x=0.05, 0.08, 0.10$). *J Magn Magn Mater*, 283 (2-3) (DEC, 2004), 375-379. ISSN: 0304-8853.
- Lines, M. & Glass, A. (1977). *Principles and Applications of Ferroelectrics and Related Materials*, Clarendon Press, ISBN: 0-19-851286-4. Oxford.
- Liu, P. F.; Wang, J. L.; Meng, X. J.; Yang, J. Dkhil B. & Chu, J. H. (2010). Huge electrocaloric effect in Langmuir-Blodgett ferroelectric polymer thin films. *New J. Phys.* 12, 023035/1-8. ISSN: 1367-2630.

- Lu, S. G., Xu, Z. K. & Chen, H. (2005). Field-induced dielectric singularity, critical exponents, and high-dielectric tunability in [111]-oriented $(1-x)\text{Pb}(\text{Mg}_{1/3}\text{Nb}_{2/3})\text{O}_3-x\text{PbTiO}_3$ ($x=0.24$) *Phys Rev B* 72 (5) (AUG, 2005), 054120/1-4. ISSN: 1098-0121.
- Mathur, N. & Mischenko, A. (2006). Solid state electrocaloric cooling devices and methods. World Patent, WO 2006/056809.
- Mischenko, A. S.; Zhang, Q.; Scott, J. F.; Whatmore, R. W. & Mathur, N. D. (2006). Giant electrocaloric effect in thin-film $\text{PbZr}_{0.95}\text{Ti}_{0.05}\text{O}_3$. *Science*, 311 (5765) (MAR, 2006), 1270-1271. ISSN: 0036-8075.
- Neese, B.; Chu, B. J.; Lu, S. G.; Wang, Y.; Furman, E. & Zhang, Q. M. (2008). Large electrocaloric effect in ferroelectric polymers near room temperature. *Science*, 321 (5890) (AUG, 2008), 821-823. ISSN: 0036-8075.
- Neese, B. Ph.D. Dissertation, The Pennsylvania State University, 2009.
- Newnham, R. E. (2005). *Properties of Materials: anisotropy, symmetry, structure*. Oxford University Press, ISBN: 019852076X/ISBN-13: 9780198520764. Oxford.
- Nolas, G.; Sharp, J. & Goldsmid, H. (2001). *Thermoelectrics*, Springer-Verlag, ISBN: 978-3-540-41245-8. Berlin.
- Pecharsky, A. O.; Gschneidner Jr., K. A. & Perchinsky, V. K. (2003). The giant magnetocaloric effect of optimally prepared $\text{Gd}_5\text{Si}_2\text{Ge}_2$. *J Appl Phys*, 93 (8) (APR, 2003), 4722-4728. ISSN: 0021-8979.
- Pecharsky, V. K.; Holm, A. P.; Gschneidner Jr., K. A. & Rink, R. (2003). Massive magnetic-field-induced structural transformation in Gd_5Ge_4 and the nature of the giant magnetocaloric effect. *Phys Rev Lett*, 91 (19) (NOV, 2003), 197204/1-4. ISSN: 0031-9007.
- Pecharsky, V. K.; Moorman, J. O. & Gschneidner Jr., K. A. (1997). A 3-350 K fast automatic small sample calorimeter. *Rev Sci Instrum*, 68 (11) (NOV, 1997), 4196-4207. ISSN: 0034-6748.
- PI Ceramic website: www.piceramic.de/site/piezo_002.html (accessed: January, 2009).
- Provenzano, V.; Shapiro, A. J. & Shull, R. D. (2004). Reduction of hysteresis losses in the magnetic refrigerant $\text{Gd}_5\text{Ge}_2\text{Si}_2$ by the addition of iron. *Nature*, 429 (6994) (JUN, 2004), 853-857. ISSN: 0028-0836.
- Sinyavsky, Y. V. & Brodyansky, V. (1992). Experimental testing of electrocaloric cooling with transparent ferroelectric ceramic as a working body. *Ferroelectrics*, 131 (1-4) (1992), 321-325. ISSN: 0015-0193.
- Sinyavsky, Y. V.; Pashkov, N. D.; Gorovoy, Y. M. & Lugansky, G. E. & Shebanov, L. (1989). The optical ferroelectric ceramic as working body for electrocaloric refrigeration. *Ferroelectrics*, 90, 213-217. ISSN: 0015-0193.
- Spanner, D. C. (1951). The Peltier effect and its use in the measurement of suction pressure. *J. Experm. Botany*, 2 (5), 145-168. ISSN: 0022-0957.
- Spichkin, Y. I.; Derkach, A. V.; Tishin, A. M.; Kuz'min, M. D.; Chernyshov, A. S.; Gschneidner Jr., K. A. & Pecharsky, V. K. (2007). Thermodynamic features of magnetization and magnetocaloric effect near the magnetic ordering temperature of Gd. *J. Magn Magn Mater*, 316 (2) (SEP, 2007), e555-e557. ISSN: 0304-8853.
- Tocado, L.; Palacios, E. & Burriel, R. (2005). Direct measurement of the magnetocaloric effect in $\text{Tb}_5\text{Si}_2\text{Ge}_2$. *J Magn Magn Mater*, 290-291 (Part 1, SP. Iss SI) (APR, 2005), 719-722. ISSN: 0304-8853.

- Tuttle, B. A. & Payne, D. A. (1981). The effect of microstructure on the electrocaloric properties of $\text{Pb}(\text{Zr},\text{Sn},\text{Ti})\text{O}_3$ ceramics. *Ferroelectrics*, 37 (1-4) (1981), 603-606. ISSN: 0015-0193.
- Wiseman, G. G. & Kuebler, J. K. (1963). Electrocaloric effect in ferroelectric Rochelle salt. *Phys Rev*, 131 (5) (1963), 2023-2027. ISSN: 0013-899X.
- Wood, M. E. & Potter, W. H. (1985). General analysis of magnetic refrigeration and its optimization using a new concept: maximization of refrigerant capacity. *Cryogenics*, 25 (12) (DEC, 1985), 667-683. ISSN: 0011-2275.
- Xiao, D. Q.; Wang, Y. C.; Zhang, R. L.; Peng, S. Q.; Zhu, J. G. & Yang, B. (1998). Electrocaloric properties of $(1-x)\text{Pb}(\text{Mg}_{1/3}\text{Nb}_{2/3})\text{O}_3-x\text{PbTiO}_3$ ferroelectric ceramics near room temperature. *Mater Chem Phys*, 57 (2) (DEC, 1998), 182-185. ISSN: 0254-0584.
- Yao, H.; Ema, K. & Garland, C. W. (1998). Nonadiabatic scanning calorimeter. *Rev Sci Instrum*, 69 (1) (JAN, 1998), 172-178. ISSN: 0034-6748.
- Ye, Z. G. & Schmid, H. (1993). Optical dielectric and polarization studies of the electric field-induced phase transition in $\text{Pb}(\text{Mg}_{1/3}\text{Ng}_{2/3})\text{O}_3$ [PMN]. *Ferroelectrics*, 145 (1) (AUG, 1993), 83-108. ISSN: 0015-0193.

IntechOpen



Ferroelectrics

Edited by Dr Indrani Coondoo

ISBN 978-953-307-439-9

Hard cover, 450 pages

Publisher InTech

Published online 14, December, 2010

Published in print edition December, 2010

Ferroelectric materials exhibit a wide spectrum of functional properties, including switchable polarization, piezoelectricity, high non-linear optical activity, pyroelectricity, and non-linear dielectric behaviour. These properties are crucial for application in electronic devices such as sensors, microactuators, infrared detectors, microwave phase filters and, non-volatile memories. This unique combination of properties of ferroelectric materials has attracted researchers and engineers for a long time. This book reviews a wide range of diverse topics related to the phenomenon of ferroelectricity (in the bulk as well as thin film form) and provides a forum for scientists, engineers, and students working in this field. The present book containing 24 chapters is a result of contributions of experts from international scientific community working in different aspects of ferroelectricity related to experimental and theoretical work aimed at the understanding of ferroelectricity and their utilization in devices. It provides an up-to-date insightful coverage to the recent advances in the synthesis, characterization, functional properties and potential device applications in specialized areas.

How to reference

In order to correctly reference this scholarly work, feel free to copy and paste the following:

S. G. Lu, B. Rozic, Z. Kutnjak and Q. M. Zhang (2010). Electrocaloric Effect (ECE) in Ferroelectric Polymer Films, *Ferroelectrics*, Dr Indrani Coondoo (Ed.), ISBN: 978-953-307-439-9, InTech, Available from: <http://www.intechopen.com/books/ferroelectrics/electrocaloric-effect-ece-in-ferroelectric-polymer-films>

INTECH
open science | open minds

InTech Europe

University Campus STeP Ri
Slavka Krautzeka 83/A
51000 Rijeka, Croatia
Phone: +385 (51) 770 447
Fax: +385 (51) 686 166
www.intechopen.com

InTech China

Unit 405, Office Block, Hotel Equatorial Shanghai
No.65, Yan An Road (West), Shanghai, 200040, China
中国上海市延安西路65号上海国际贵都大饭店办公楼405单元
Phone: +86-21-62489820
Fax: +86-21-62489821

© 2010 The Author(s). Licensee IntechOpen. This chapter is distributed under the terms of the [Creative Commons Attribution-NonCommercial-ShareAlike-3.0 License](#), which permits use, distribution and reproduction for non-commercial purposes, provided the original is properly cited and derivative works building on this content are distributed under the same license.

IntechOpen

IntechOpen